ORIGINAL ARTICLE

Living on the edge: Ecological and genetic connectivity of the spiny-footed lizard, *Acanthodactylus aureus*, confirms the Atlantic Sahara desert as a biogeographic corridor and centre of lineage diversification

Guillermo Velo-Antón[1] [iD] | Fernando Martínez-Freiría[1] | Paulo Pereira[1] |
Pierre-André Crochet[2] | José Carlos Brito[1,3]

[1]CIBIO/InBIO, Centro de Investigação em Biodiversidade e Recursos Genéticos da Universidade do Porto, Instituto de Ciências Agrárias de Vairão, R. Padre Armando Quintas n° 7, 4485-661, Vairão, Portugal

[2]CEFE UMR 5175, CNRS - Université de Montpellier - Université Paul-Valéry Montpellier − EPHE, Montpellier cedex 5, France

[3]Departamento de Biologia da, Faculdade de Ciências da, Universidade do Porto, Porto, Portugal

Correspondence
Guillermo Velo-Antón, CIBIO/InBIO, Centro de Investigação em Biodiversidade e Recursos Genéticos da Universidade do Porto, Instituto de Ciências Agrárias de Vairão, R. Padre Armando Quintas n° 7, 4485-661, Vairão, Portugal.
Email: guillermo.velo@cibio.up.pt

Funding information
Fundação para a Ciência e a Tecnologia, Grant/Award Number: PTDC/BIA-BEC/099934/2008, PTDC/BIA-BIC/2903/2012, IF/01425/2014, IF/00459/2013, PD/BD/128492/2017; FEDER funds through the Operational Programme for Competitiveness Factors - COMPETE, Grant/Award Number: FCOMP-01-0124-FEDER-008917/028276

Editor: Krystal Tolley

Abstract

Aim: Climatic fluctuations in northern Africa substantially changed the extent of the Sahara desert and Saharan species' ranges. Yet, the region contained areas of climatic stability. We test the hypothesis that the Atlantic Sahara was a stable corridor, connecting ecoregions, for the spiny-footed lizard *Acanthodactylus aureus*.

Location: Africa, Saharan Atlantic coastal desert.

Methods: We combined ecological modelling and phylogeographic and population genetic analyses. Ecological models for past and current conditions were used to predict climatically stable areas for the species over time. Genetic analysis, including for three mitochondrial fragments (12S, Cytb and COI), one nuclear gene (C-mos) and 18 microsatellite markers, were used to unveil patterns of genetic structure and diversity, and gene flow dynamics within *A. aureus*.

Results: Three mtDNA allopatric lineages diversified during the Pliocene-Pleistocene along the Atlantic Sahara. Two main areas of high climatic stability largely fit the regions with highest mtDNA diversity. Mito-nuclear discordances along some coastal regions indicate evidence of gene flow between lineages, which are likely mediated by population expansions and male-biased dispersal. Several geographical barriers to gene flow were also identified.

Main conclusion: This study highlights the role of the Atlantic Sahara ecoregion both as a centre of lineage diversification and as a occasional suitable corridor within the Sahara desert. Population retractions and expansions resulting from climatic oscillations during the Pleistocene, facilitated allopatric diversification and genetic introgression processes along this region, whereas stable geographical barriers limited gene flow dynamics.

KEYWORDS
Atlantic Sahara, biodiversity corridor, climatic stability, genetic structure, lizard, phylogeography

1 | INTRODUCTION

Understanding how climate and geographical features have promoted species diversification, distributions and patterns of genetic diversity is a fundamental task in biogeography (Lomolino, Riddle, Brown, & Brown, 2006). Desert regions constitute seemingly homogeneous areas that can be used to evaluate the effects of climatic oscillations on biodiversity patterns (Ward, 2009). Many dry deserts have experienced numerous dry-humid cycles during the Quaternary (e.g. Hesse, Magee, & van der Kaars, 2004; Stuut & Lamy, 2004; Tchakerian & Lancaster, 2002) inducing range shifts that have shaped current biodiversity patterns. Drier periods were unsuitable for mesic, more water-dependent species, leading to range retractions to mild areas (e.g. Duckett, Wilson, & Stow, 2013) and subsequent diversification processes (e.g. Douady, Catzeflis, Raman, Springer, & Stanhope, 2003; Graham, Jaeger, Prendini, & Riddle, 2013) and local extinctions (e.g. Watrin, Lézine, & Hély, 2009). Conversely, demographic expansions and subsequent gene flow between lineages in secondary contact zones mainly occurred during more humid periods (e.g. Strasburg, Kearney, Moritz, & Templeton, 2007). On the contrary, xeric species could expand their ranges with increasing aridity (e.g. Kearns, Joseph, Toon, & Cook, 2014) and experience range fragmentation leading to diversification in the more humid periods (e.g. Carranza, Arnold, Geniez, Roca, & Mateo, 2008). These evolutionary processes may be reduced or absent in areas showing climatic stability throughout the periods of fluctuations. Coastal areas in desert environments, where the ocean plays a crucial role as a stabilizing factor, may buffer the otherwise extreme conditions and climatic shifts (Ward, 2009).

The Sahara Desert has suffered profound climatic fluctuations, where Saharan endemics and isolated populations from neighbouring ecoregions persisted by adapting to new environments or by tracking suitable climatic conditions (see Brito et al., 2014). Climatically stable areas allowed species to survive within the Sahara. These climatically stable areas are mostly located in mountains that currently hold rich communities and contain about half of the Sahara-Sahel endemic vertebrate species (e.g. Gonçalves et al., 2012; Trape, 2009; Vale, Pimm, & Brito, 2015). Within the region, the Saharan Atlantic coastal desert (hereafter, Atlantic Sahara) may have acted as both a climatic refuge and a putative corridor (Brito et al., 2014). The Atlantic Ocean's proximity creates different climatic conditions when compared to inland areas at the same latitudes: coastal temperatures are milder and prone to less variation, and despite the low precipitation, the sea fog and dew help vegetation growth (Dinerstein et al., 2017). These environmental conditions provide continuous distributions along the area for several taxonomical groups (Brito et al., 2016). A number of taxa are fully or nearly endemic to the Atlantic Sahara, such as the reptiles *Acanthodactylus aureus* (Crochet, Geniez, & Ineich, 2003) and *Tarentola chazaliae* (Trape, Trape, & Chirio, 2012), and the mammals *Crocidura tarfayaensis* (Vogel et al., 2006) and *Gerbillus occiduus* (Ndiaye et al., 2012).

This study aims to test for the first time the hypothesis that the Atlantic Sahara serves as a biodiversity corridor, which relies on the more stable climatic conditions induced by the proximity of the sea during climatic oscillations (Brito et al., 2014). We investigate this hypothesis using the spiny-footed lizard *A. aureus*, through ecological modelling and genetic analyses. Specifically, we evaluate using *A. aureus* as our model species: (1) if there have been climatically stable habitats; (2) if current patterns of genetic population structure were mainly shaped by vicariance in distinct refugia, by continuous gene flow and isolation by distance, or by an interplay of both mechanisms. If the Atlantic Sahara is indeed a biodiversity corridor, with continuous availability of suitable habitats for dispersal, we expect the study species to show: (1) a continuous stable climatic area and continuous gene flow across the area through time, with a pattern of isolation by distance but (2) little or no break in the genetic structure across the area. The region is also characterized by numerous hydrological elements that can act as landscape barriers, such as the basin of As-Saguia Al-Hamrah or the Drâa valley. If these elements play a role as barriers despite the climatic continuity and stability of the area, species are expected to display spatial and temporal interruptions in gene flow. Our integrative analyses provide insights regarding the role of a putative biodiversity corridor on the western extreme of the world's largest warm desert.

2 | MATERIALS AND METHODS

2.1 | Study area, organism and sampling

Our study region encompasses the Saharan Atlantic coastal desert ecoregion (Dinerstein et al., 2017), and adjacent inland regions (Figure 1; Text S1.1 in Appendix S1).

Acanthodactylus aureus is nearly endemic to the Atlantic Sahara, with a NW African origin (Tamar et al., 2016). It is continuously distributed along the Atlantic coast, from the valley of Oued Sous (Morocco) to the Baie of Levrier (Mauritania), spreading more than 100 km inland along As-Saguia Al-Hamrah (Morocco) and with few records in coastal Senegal. The species occupies coastal dunes and other sandy habitats. It has a continuous distribution along the coast of the study area, with some patchy inland populations in sandy habitats (Sindaco & Jeremčenko, 2008).

We used a total of 130 georeferenced tissue samples covering most of the known distribution of the species (Figure 1; Table S2.1 in Appendix S2), including 125 collected by the authors during the period of 2004–2014 and five obtained from ethanol preserved specimens (from the Museum Nationale d'Histoire Naturelle, Paris and the Zoological Research Museum Alexander Koenig, Bonn).

2.2 | Modelling of climatic suitability

A total of 81 presence records of *A. aureus* (corresponding to the 130 tissue samples) were tested for spatial clustering to reduce
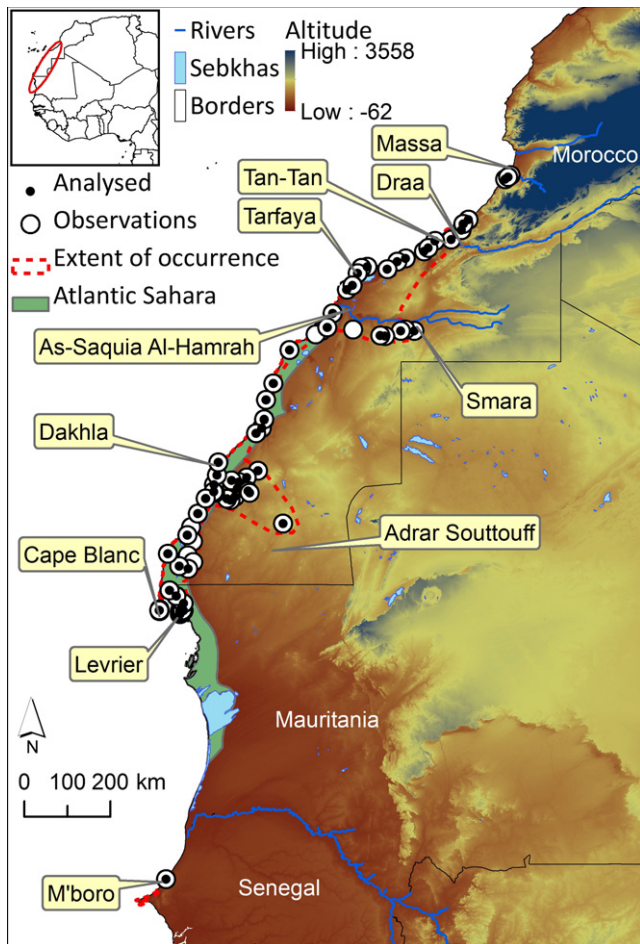
FIGURE 1 Map of sampling localities used in this study. White circles are observations of *Acanthodactylus aureus*, whereas filled circles denote analysed samples. The red oval depicted in the inset of this figure represents the location of the study area in north-west Africa. The Atlantic Sahara ecoregion is represented in a green polygon and the distribution of the main water bodies are depicted in blue. The red dashed line represents the present distribution of *A. aureus*. Relevant localities used along the text are also indicated in the map

sampling bias in ecological procedures (Boria et al., 2014). Spatial filtering from clusters of presences was assessed by the "Average Nearest Neighbour" tool of ArcGIS (ESRI, 2006). The final low clustering distribution dataset (nearest neighbour ratio = 0.582, z-score = −6.641) included 70 presence records (average distance of 0.2°).

For current conditions, five slightly correlated ($R < .61$) climatic variables were chosen for modelling purposes (see Text S1.2; Table S2.2). Variables at 30 arc-seconds (~1 × 1 km) were downloaded from WorldClim (http://www.worldclim.org; Hijmans, Cameron, Parra, Jones, & Jarvis, 2005). For past conditions, the same five climatic variables were downloaded from WorldClim for the Last Interglacial (LIG; ~120,000–140,000 years BP; Otto-Bliesner, Marshall, Overpeck, Miller, & Hu, 2006), the Last Glacial Maximum (LGM; ~21,000 years BP) and the middle Holocene (midHol; 6,000 years BP) periods (Text S1.2).

Ecological models were built using BIOMOD 2 (Thuiller, Georges, & Engler, 2012). Two regression-based (GLM, generalized linear models; and GAM, generalized additive models) and two machine learning-based algorithms (ANN, artificial neural networks; and MAXENT, maximum entropy) were chosen to reduce the uncertainties associated with modelling techniques (Wiens, Stralberg, Jongsomjit, Howell, & Snyder, 2009). All models were run using default parameters (Thuiller et al., 2012).

Presence records for each dataset were imported into BIOMOD within a study area consisting of a 300 km buffer from the coastline (extending from 31.5° to 13.3°N; Figure 1). This area was chosen following calibration to avoid biases when selecting pseudo-absences and selecting additional areas as potential climatic refugia (Anderson & Raza, 2010). Five pseudo-absences datasets were created, each one with 10,000 random data points, using regression and machine-learning algorithms (Barbet-Massin, Jiguet, Albert, & Thuiller, 2012). The number of pseudo-absences was chosen to have the same weight as presence data during model calibration (i.e. prevalence = 0.5).

Ten model replicates were run for each of the five pseudo-absences datasets and for each of the four algorithms. Presence data for each replicate were selected randomly by cross-validation, using 80% of data for training (Text S1.3). The contributions of the climatic variables to the consensus models were evaluated by averaging the relative contribution to individual model replicates (e.g. Martínez-Freiría, Velo-Antón, & Brito, 2015).

Individual model replicates were projected to past climatic conditions (midHol, LGM and LIG). Projections were assessed using clamping masks (Elith, Kearney, & Phillips, 2010). Individual model replicates were then added to generate a consensus model of species presence under each past period. Consensus projections were spatially assessed by displaying the variation coefficients among replicates (Thuiller et al., 2012).

Consensus models and projections to past climatic conditions were converted to binary (i.e. presence/absence) using the optimized threshold from the receiver operating characteristics plot that maximizes sensitivity and specificity (see Liu, Berry, Dawson, & Pearson, 2005). Binary consensus models for past and current conditions were overlapped in ARCGIS to identify stable climatic areas over time (i.e. common potential areas of occurrence in different time periods which could thus serve as refugia; Carnaval, Hickerson, Haddad, Rodrigues, & Moritz, 2009).

2.3 | DNA extraction, amplification, sequencing and genotyping

Genomic DNA extractions were performed from tail tips stored in ethanol using QIAGEN's EasySpin Kit and stored at −20°C prior to amplification. The success of DNA extractions was evaluated by electrophoresis on 0.8% agarose gels stained with Gel Red, in TBE 0.5x buffer.

A first screening of the genetic diversity and structure was performed by amplifying and sequencing one mitochondrial marker (12S

rRNA; 362 base pairs) for the entire dataset. Main mtDNA lineages were identified using TCS 1.2.1 (Clement, Posada, & Crandall, 2000), which produced 19 haplotypes, structured in three main haplotype networks. A subset of 50 samples was selected to represent the distribution area and all main mitochondrial lineages. This subset was amplified and sequenced for two additional mtDNA markers: Cytochrome-b (Cytb, 383 bp) and cytochrome oxidase I (COI, 832 bp); and one nuclear marker, the nuclear fragment oocyte maturation factor MOS (C-mos, 511 bp). Polymerase chain reactions (PCRs) were performed in 10 µl reaction volumes comprising 5 µl of MyTaq (MyTaq™ Mix; Bioline), 3 µl of pure water, 0.5 µl of reverse and forward primers and 1 µl of template DNA. PCR products were cleaned using ExoSAP, and the purification and sequencing was outsourced to Beckman Coulter Genomics. Amplified mitochondrial fragments were sequenced for the forward strand, whereas the nuclear fragment was sequenced in both directions. Primers and PCR conditions are listed in Tables S2.3 and S2.4 respectively. Sequences were edited and aligned in GENEIOUS Pro 4.8.5 using the GENEIOUS alignment tool, applying the default settings.

All 130 samples were genotyped for a set of 22 microsatellites that was developed for the *Acanthodactylus scutellatus* species group (Lopes et al., 2015). Of those, 21 loci amplified consistently and were polymorphic for *A. aureus*. PCRs were performed in 10 µl reaction volumes, including: 5 µl of Master Mix, 3 µl of pure water, 1 µl of primer mix and 1 µl of template DNA. Loci were combined into four multiplexes using varying amounts of primer concentrations (see Tables S2.4 and S2.5). Microsatellites PCR products were later separated by capillary electrophoresis on an automatic sequencer ABI3130xl Genetic Analyzer (AB Applied Biosystems), using 1 µl of amplification product and 10 µl of formamide + 75-400 (-250) LIZ NEW size standard. All PCRs were performed in a Biometra T-professional Thermocycler and obtained PCR products were checked by electrophoresis on 2% agarose gels stained with Gel Red, using a mass DNA ladder (NZYDNA Ladder V). Allele calling was performed in GENEMAPPER 4.0 (Applied Biosystems) and manually checked twice.

2.4 | Phylogenetic analyses and estimation of divergence times

Phylogenetic analysis using Bayesian inference (BI) was performed on the 50 samples that were sequenced for the four genetic fragments (c. 2,088 bp; Table S2.1). The best-fitting model of nucleotide substitutions for each gene was determined with JMODELTEST 2.1.5 (Darriba, Taboada, Doallo, & Posada, 2012), using the Bayesian information criterion (BIC). The models indicated as best were TRN+I+G for 12S, Cytb and C-mos and HKY+I for COI.

BI analyses were performed with BEAST 1.8.0 (Drummond, Suchard, Xie, & Rambaut, 2012), with unlinked substitution models for each gene. Absolute divergence times of *A. aureus* major lineages were estimated using the mean substitution rates and the standard error of the 12S and Cytb mitochondrial regions obtained from a fully calibrated phylogeny of a closely related lacertid group

(Carranza & Arnold, 2012). A normal distribution was used for the substitution rates (ucld.mean of 12S: 0.00553, SD: 0.00128; ucld.mean of Cytb: 0.0164, SD: 0.00317). To account for variability in the heterozygote positions for the nuclear partition, the .xml file was modified to "Ambiguities = true". A log–relaxed clock and a coalescence constant size model were used as tree priors. Three independent MCMC runs of 100 million generations were implemented, sampling every 10,000 generations and 10% of the trees were discarded as burn-in. The convergence of chains and effective sample sizes (ESSs) for all parameters was verified using TRACER 1.6. (http://tree.bio.ed.ac.uk/software/tracer/ ESSs higher than 300 for all parameters). Log and tree files of the three independent runs were combined using LOGCOMBINER. The subsequent maximum clade credibility summary tree with posterior probabilities for each node, using the median values, was obtained in TREEANOTATOR (both available in the BEAST package). The resulting tree was visualized and edited with FIGTREE 1.4.1 (http://tree.bio.ed.ac.uk/software/figtree). Nodes were considered strongly supported if they received a posterior probability (PP) $\geq$ 0.95. Haplotype networks were constructed for the mtDNA fragment with a good sampling coverage (12S; $N = 129$; Table S2) and the nuclear gene (Cmos; $N = 51$; Table S2) using TCS, with a 95% parsimony threshold. PHASE, implemented in DNASP 5.10.01 (Librado & Rozas, 2009), was used to phase the nuclear data. The algorithm was run five times, for 10,000 iterations, with a burn-in of 1,000. The most probable reconstructed haplotypes were used to create the haplotype network. Positions that remained unclear were treated as missing data. Calculations of sequence divergence were performed in MEGA 7 (Tamura, Stecher, Peterson, Filipski, & Kumar, 2013) for 12S based on the Kimura-2 parameter model.

2.5 | Microsatellite analyses

Potential evidences of stuttering, null alleles and allelic dropouts were assessed using MICRO-CHECKER 2.2.3 (Van Oosterhout, Hutchinson, Wills, & Shipley, 2004). Tests for genotypic linkage disequilibrium (LD) and Hardy–Weinberg equilibrium (HWE) were assessed in GENEPOP online version (http://wbiomed.curtin.edu.au/genepop/); with subsequent Bonferroni correction in both cases, following the method explained in Lopes et al. (2015).

Bayesian clustering analyses were conducted using STRUCTURE 2.3.4 (Falush, Stephens, & Pritchard, 2003). The admixture model was used, assuming correlated allele frequencies, and without incorporation of sampling localities. Ten runs were carried out for each K value, from 1 to 10 (exceeding the maximum number of groups detected with the phylogenetic analyses), with an initial burn-in of 10^6 iterations and an additional 10^7 iterations after the burn-in. STRUCTURE HARVESTER (Earl 2012) was used to estimate the optimal number of clusters (K) through the examination of Ln $p(X \mid K)$ as well as the ΔK (Evanno, Regnaut, & Goudet, 2005). Factorial correspondence analyses (FCAs) on individual genotypes were run using the program GENETIX (Belkhir, Borsa, Chikhi, Raufaste, & Bonhomme, 2004). Default options of the program were used, except that we retained more axes (8). The first FCA was run on all individuals, the

second on samples from the southern and central clade to further explore the nuclear differentiation between these two clades. Last, we computed Fst values between the three mtDNA clades using the Weir and Cockerham's estimator Θ with GENETIX. Significance of Θ values was assessed by permuting individuals between populations (1,000 permutations).

2.6 | Geographical distribution of genetic diversity

To spatially measure expected heterozygosity (H_E) and haplotype diversity (h), a non-overlapping sliding window approach was performed to avoid autocorrelation between windows. A linear model was used to summarize the geographical coordinates of the samples into a single dimension. The coefficients of the linear model were extracted and used to transform the longitude values as a function of the model. The window was configured as having a total height of one geographical degree (~90 km), with the starting middle point of the first window at the lowest transformed longitude value, and then slide by one geographical degree in order for the lower border of the second sliding window to match the higher border of the first sliding window. For each window, the number of unique haplotypes and expected H_E was assessed (h).

3 | RESULTS

3.1 | Climatic stability for *A. aureus*

A total of 123 robust replicates (TSS >0.75) were used for deriving the consensus model for *A. aureus* (Table S2.6). Percentages of correct classified validation samples were high (>91%) in all binary models. One temperature variable (bio 7) was found as most related to the species distribution in the four modelling algorithms (Table S2.6).

Probability models mostly fit the species distribution, with the exception of areas located at As-Saquia Al-Hamrah and Adrar Souttouff that were not predicted as suitable in all models (Figure S3.1 in Appendix S3). The highest values of dissimilarity between replicas were mostly located at range margins in the four algorithms (Figure S3.1). With exception of As-Saquia Al-Hamrah, Adrar Souttouff and Senegalese coast, the binary consensus models for current conditions mostly fit the distribution of *A. aureus*.

Probabilistic projections to past conditions mostly showed similar patterns across algorithms, with reduced interconnectivity between northern and southern areas predicted for almost all the periods (Figure S3.1). Accordingly, binary consensus projections to the LIG showed two disconnected areas located in between the Cape Blanc, Dakhla and Tarfaya regions. These suitable areas likely shifted northwards and became connected in the LGM but slightly disconnected in the midHol (Figure S3.2).

Consequently, two main areas of high climatic stability in the habitats occupied by *A. aureus* can be identified: one area in Tarfaya with some coastal patches spreading northwards and a larger area between Cape Blanc and north of Dakhla (Figure 2).
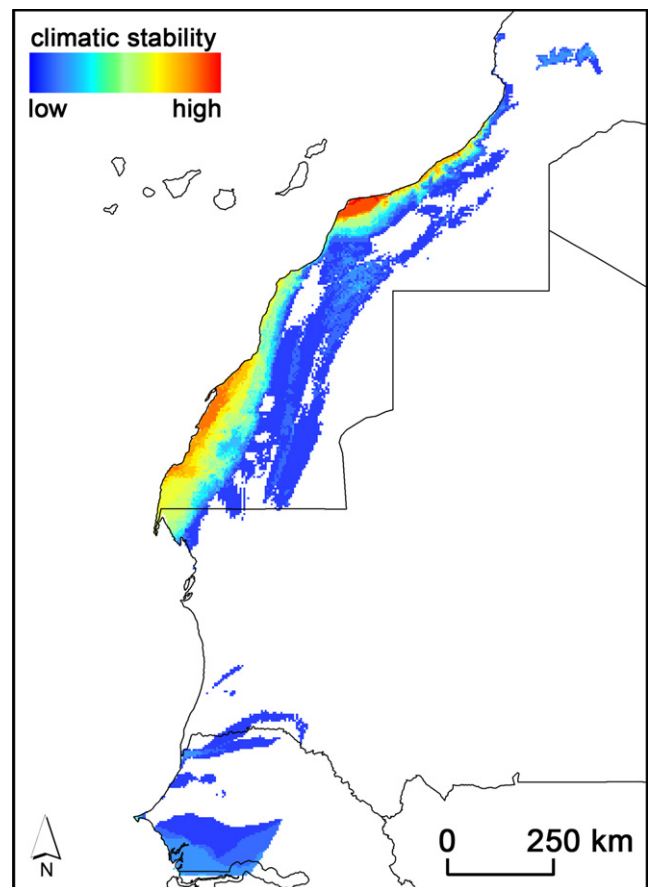

FIGURE 2 Climatic stability of suitable areas for *Acanthodactylus aureus* over time, derived from ecological models using four algorithms and respective projections to three past periods (mid-Holocene, Last Glacial Maximum and Last Interglacial). Warm colours represent higher climatic stability

3.2 | Phylogenetic analyses

The final dataset included 129 samples that were sequenced for at least one mitochondrial locus and 130 specimens genotyped for the microsatellite loci (see Table S2.1).

The BI phylogenetic analyses revealed three major geographically structured lineages within *A. aureus* (Figure 3a; Fig. S3.7): a northern lineage (*North*), including coastal individuals from the central species distribution to the north; a central-inland lineage (*C-I*), grouping some coastal individuals and the inland sampled localities; and a southern lineage (*South*), including coastal individuals from the southernmost species distribution. However, the relationships among lineages remain uncertain considering the low nodal support. The three main lineages are supported for the haplotype network constructed with 12S sequences (Figure 3b). Two nuclear (C-mos) haplotypes (haplotypes A and B) are extensively shared among the three mtDNA lineages throughout the entire distribution of *A. aureus*. Other nuclear haplotypes are also shared between lineages, but restricted to southern and central-inland populations (haplotypes C, F, H, J; Table S2.1), with other nuclear

haplotypes restricted to each main lineage (Figure 3c). The TMRCA (time to most recent common ancestor) of *A. aureus* mtDNA haplotypes can be dated to the late Pliocene, approximately 2.5 Ma (95% HPD: 0.5–3). The MRCA of the *North* (1.0 Ma; 95% HPD: 0.5–1.9) and *C-I* lineages (1.1 Ma; 95% HPD: 0.6–2.2) occurred in the early-medium Pleistocene, whereas the *South* lineage had a MRCA in the last million year (0.5 Ma; 95% HPD: 0.15–1.0) (Figure 3a). Mean genetic distances (uncorrected *P*-distances) between the three mtDNA lineages ranged from 1.2% to 1.6% (Table S2.7).

3.3 | Population analyses with microsatellites

Most of the samples were successfully amplified for all markers, with a few showing missing data (<22% of missing data overall). Markers with widespread evidences of null alleles, heterozygote deficiency and stuttering were removed, obtaining a final filtered dataset of 130 individuals and 18 markers (Table S2.1). No LD was observed in the final dataset (Table S2.8).

STRUCTURE analyses showed that the best-supported number of clusters was *K* = 2 according to the Δ*K* method (Figure S3.3): cluster K1 groups individuals from the *North* lineage; whereas cluster K2 groups individuals from *South* and *C-I* lineages, including the southernmost individuals from the *North* lineage (Figure 3b). Further structuring observed for *K* = 3 represented a third cluster within the former K1, grouping population north of the Drâa valley and some admixture with neighbouring localities from K2 (Figure S3.4). No further structure was found for higher *K*.

The FCA supported STRUCTURE results: there was a clear separation of the samples into two nuclear clusters along the first axis of the FCA (Figure 5; Figure S3.5). The first cluster (FC1 value below −1) included *North* specimens only, whereas the other cluster (FC1 values above 0) included almost all *C-I* and *South* individuals, with a few specimens carrying *North* mtDNA. A large number of specimens (mostly with the *North* mtDNA lineage) had an intermediate position along the first FCA axis (FC1 value between 0 and −1), suggesting extensive admixture. A FCA restricted to the *C-I* and *South* individuals confirmed the lack of strong differentiation between these two
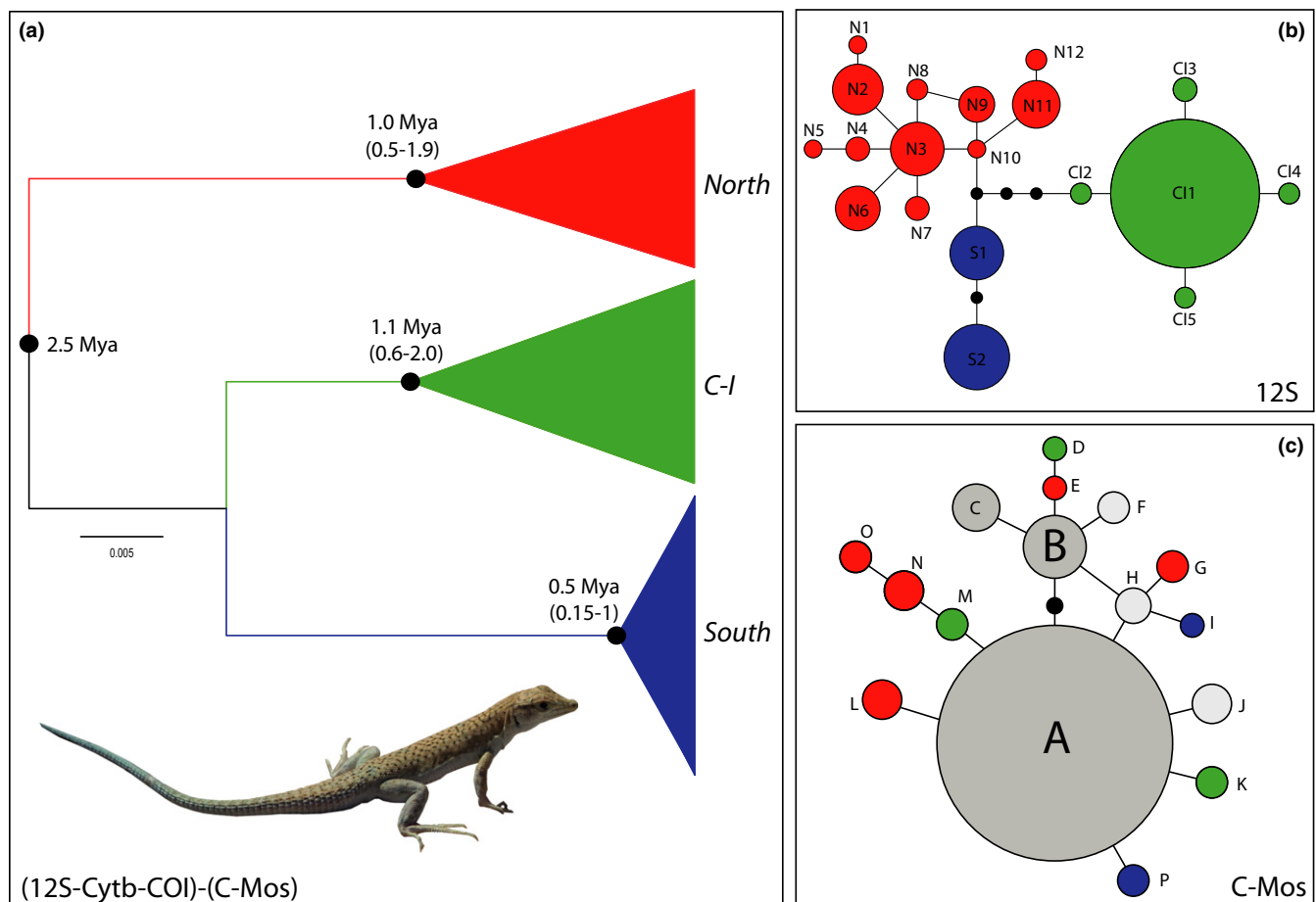

FIGURE 3 (a) Time-calibrated (Ma, 95% HPD in brackets) Bayesian phylogenetic tree for *Acanthodactylus aureus* obtained from a concatenated dataset of three mitochondrial markers (12S, Cytb and COI) and one nuclear marker (C-mos). Black dots represent posterior probabilities (*p* > .95). (b) TCS haplotype network for mtDNA (12S). (c) TCS haplotype network for nuDNA (C-mos). The three main mtDNA lineages are depicted in red (North clade), blue (C-I clade) and green (South clade). Light and dark grey denote share alleles for two and three mtDNA lineages respectively

groups (Figure S3.6). The F_{ST} value between the *C-I* and *South* individuals were significant ($p < .01$) but very small ($F_{ST} = 0.011$), further indicating very weak nuclear differentiation between these mtDNA clades.

3.4 | Geographical distribution of genetic diversity and mito-nuclear discordances

Genetic diversity in *A. aureus* is unequally distributed along the species range when comparing mtDNA (12S) and nuclear (microsatellites) patterns (Figure 4). Within the *North* lineage (windows 6, 7 and 8), northern populations show higher genetic diversity at a mtDNA level (h) than central and southern populations. Central populations (window 5) show a marked reduction in genetic diversity, with only one mtDNA haplotype (N3). Contrarily, microsatellite markers identified a more even distribution of genetic diversity, with relatively high values along the complete species range (H_E: 0.70–0.82), with the populations north of the Drâa valley showing the lowest values (H_E: 0.7).

Plotting FC1 values against latitude (Figure S3.5) revealed that nuclear genetic population structure is driven by geography. The widespread southern nuclear cluster occurs over 1,000 km from Senegal to the northern Atlantic Sahara (50 km S of Laâyoune), with little sign of genetic structuring. The *North* cluster occupies the northern edge of the species distribution from the Souss valley

(Agadir) to the Draa valley (Tan-Tan). In between Tan-Tan and Laâyoune an extensive zone of admixture includes over 300 km of the coastal distribution of the species.

The transition between the *North* and *C-I* mtDNA clades is displaced toward the south compared with the nuclear transition (Figures 4 and 5), resulting in a cyto-nuclear discordance of over 200 km (between 50 km S of Laâyoune and 100 km S of Boujdour) where all specimens have *North* mtDNA lineage in a typical southern-cluster nuclear background. In addition, one specimen close to Tan-Tan has a *C-I* haplotype in a mostly northern nuclear background.

4 | DISCUSSION

The integration of ecological modelling and phylogeographic analyses in the Saharan endemic spiny-footed lizard allowed us to test if there was an ecological corridor along the Atlantic Sahara. This study highlights this ecoregion both as a centre of lineage diversification and as a biogeographic corridor within the Sahara desert. Allopatric climatic refugia facilitated the diversification within *A. aureus*, whereas subsequent population expansions from stable climatic areas lead to genetic introgression and secondary contact zones along the Atlantic Sahara. We also identified stable geographical barriers to gene flow between genetic groups.
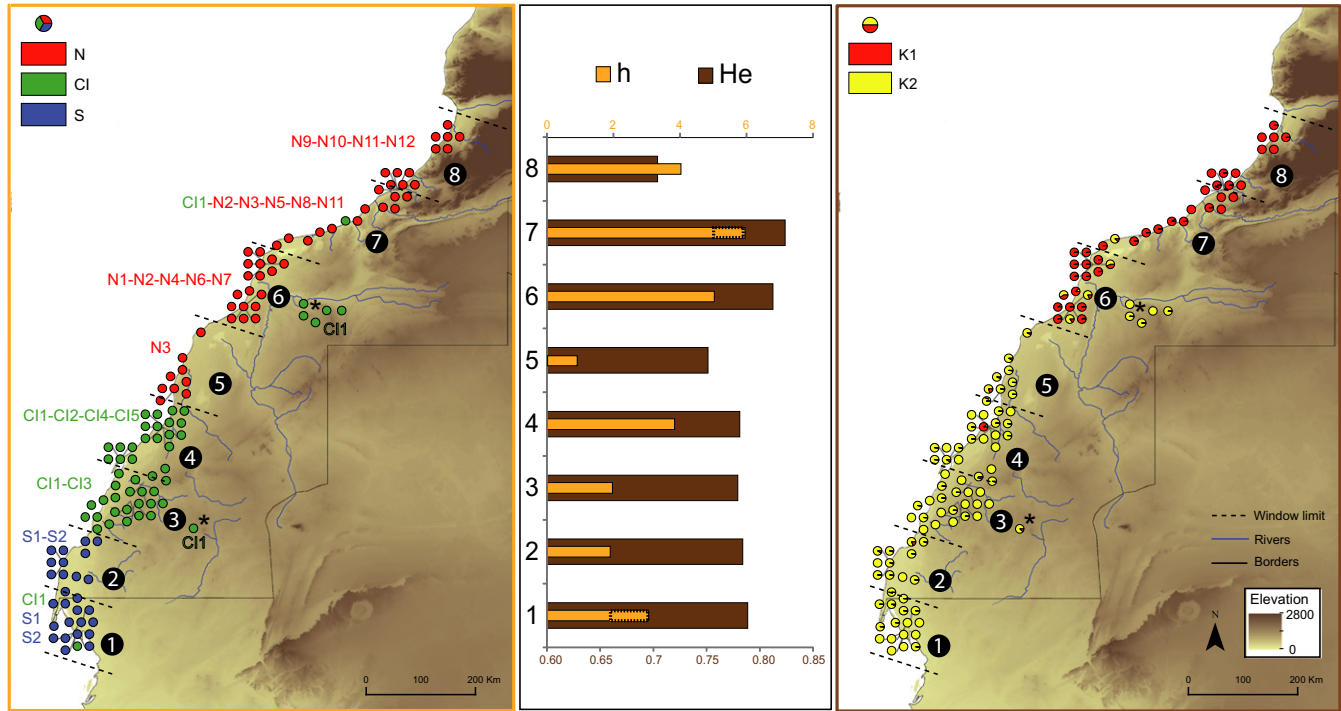

FIGURE 4 Left panel: genetic structure within *Acanthodactylus aureus* inferred with mtDNA marker (12S) using a TCS haplotype network. The three main lineages are depicted in red (North clade), blue (C-I clade) and green (South clade) for both the samples and the haplotypes. Central panel: genetic diversity (haplotype diversity, h; and expected heterozygosity, H_E) obtained for each of the eight windows created using a non-overlapping sliding window approach. Right panel: genetic structure of *A. aureus* inferred with 18 microsatellite markers using STRUCTURE. Colours represent the two main genetic demes. The eight windows are represented with numbers in a black dots and separated by dashed black lines along the study area. Asterisks denote individuals from inland populations removed from the sliding window analysis
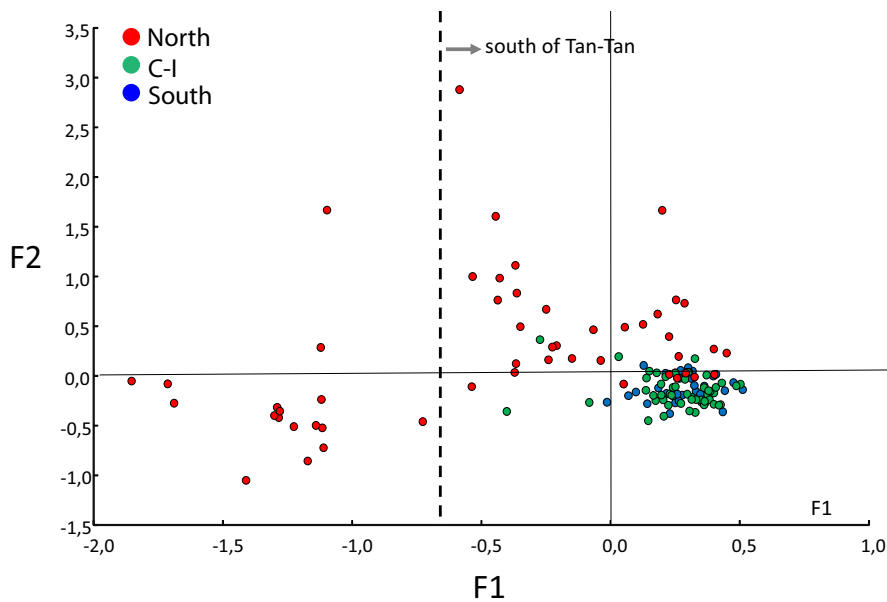
FIGURE 5 Factorial correspondence analyses (FC1 and FC2) for all genotyped individuals of *Acanthodactylus aureus*. The dashed line indicates the separation between individuals located north and south of Tan-Tan. The three main lineages are depicted in red (North clade), blue (C-I clade) and green (South clade)

4.1 | Atlantic Sahara as a centre of diversification

This study reveals that vicariance was most likely the main evolutionary process driving the current structure of genetic diversity in *A. aureus*. Range fragmentation, probably in the late Pliocene, generated a deep latitudinal genetic structure evident in both mtDNA lineages and nuclear genetic clusters. The palaeoclimatic reconstructions are concordant with the genetic results obtained for *A. aureus*, as the two disjoint areas of high climatic stability largely correspond to the current genetic structure recovered for this species. These areas provide support for past isolation events in two allopatric refugia: Tarfaya for northern populations and Dakhla for southern-central populations. Climatic oscillations may have temporarily restricted *A. aureus* to these areas, impeding gene flow between populations sheltered in both climatic stable areas and leading to allopatric diversification.

Across the Atlantic Sahara, hydrological elements potentially acted as geographical barriers disconnecting the stable suitable habitats during the LIG and mid-Holocene. Regional precipitation was higher in the LIG than in current conditions (Otto-Bliesner et al., 2006), and then decreased during the LGM and increased again in the last humid period (mid-Holocene), before the rapid installation of warmer and drier conditions. A prominent east-west oriented hydrological network may have favoured further isolation within climatic refugia. Lack of incorporation of other factors in the modelling approach (e.g. non-climatic variables; Alvarado-Serrano & Knowles, 2014) might have precluded the identification of microrefugia for these lineages (Worth, Williamson, Sakaguchi, Nevill, & Jordan, 2014). Yet, it is difficult to explain the origin of the mtDNA lineages *South* and *C-I* as these patterns are not reflected in the nuclear markers. Two alternative hypothesis can apply: (1) the two mtDNA clades result from a further vicariance event somewhere in the southern Atlantic Sahara, the effects of which has been erased by (presumably male-biased) dispersal (as in all Lacertidae studied to

date, see Ferchaud et al., 2015); and (2) the two mtDNA clades result from a coalescence process of isolation-by-distance without any break in gene flow (e.g. Irwin, 2002).

4.2 | Atlantic Sahara as a dispersal corridor for *A. aureus*

High levels of gene flow across *A. aureus* populations support the Atlantic Sahara ecoregion as a dispersal corridor through the Sahara during climatic fluctuations. Our integrative approach suggests a scenario of demographic changes (i.e. population expansions during past climatic oscillations) resulting in extensive admixture between the two main groups. While incomplete lineage sorting might explain the lack of genetic structure for the nuclear marker, the geographical pattern of microsatellite population structure shows extensive admixture between the two main evolutionary lineages over the northern half of the Atlantic Sahara. This pattern of population expansion is supported by the palaeoclimatic reconstructions (Figure S3.2) that show a wide distribution of *A. aureus* during LGM, mid-Holocene and present times.

The distribution of genetic diversity at mtDNA level supports the previously identified stable climatic areas, where the retention of the highest genetic diversity is expected (e.g. Carnaval et al., 2009; Martínez-Freiría et al., 2015). The distribution of mtDNA diversity is spatially biased, with northern and some central populations harbouring most diversity, with a clear reduction across central populations. This is exemplified in window 5, where a single haplotype was found (Figure 4). The pattern of genetic diversity observed in central populations from windows 5 and 6 help clarify the directionality of population expansions. The unequal distribution of genetic diversity would fit the suggested model of historical population expansion of *North* lineage along a north–south axis. Both males and females would colonize a previously uninhabited area due to unsuitable climatic conditions that previously acted as a climatic barrier, whereas

inland populations from Smara and Adrar Souttouff were likely colonized from central populations (Figure 2). On the other hand, the high levels of nuclear genetic diversity observed in window 5 (compared to mtDNA diversity), where lizards maintain the mitochondria of *North* lineage while being fully assigned to the southern-central genetic deme, suggests a more recent south-north population expansion.

4.3 | Origin of cytonuclear discordance

Our work adds to a long list of previous studies documenting extensive cytonuclear discordance following introgression and admixture (see Toews & Brelsford, 2012). As pointed out by these authors, it is often difficult to disentangle the role of selective processes (adaptive introgression of mtDNA variants) and neutral demographic processes in generating discordance, although massive discordance as observed here (complete mtDNA introgression without detectable nuclear introgression) is often hypothesized to involve selective rather than neutral processes. Bonnet, Leblois, Rousset, and Crochet (2017) found that neutral processes are generally unable to generate strong discordance when discordance is measured across the global range of populations involved. However, in the context of moving hybrid zones, neutral processes can generate strong discordances that are geographically restricted near the front of the expansion waves (Boursot and Melo-Ferreira pers. com.). In addition, the number and type of nuclear markers we used does not allow estimating the level of nuclear introgression, and thus the amount of discordance.

4.4 | Biogeographic barriers and contemporary genetic structure in *A. aureus*

The main biogeographic barrier identified along the *A. aureus* distribution is situated in Mauritania, where a large gap, south of Levrier, has been confirmed by numerous field expeditions. Interestingly, ENMs predicted a low climatically stable area for *A. aureus* in this region. The only available sample south of this gap has been assigned to the *South* lineage and the southern-central genetic deme). This could either suggest an isolated relict population geographically disconnected from the *A. aureus* main range by unsuitable climatic habitat during recent times, or, less likely, by accidental introductions to North Senegal where the species presence has been known for many years (see Crochet et al., 2003).

Several rivers might have constituted historical geographical barriers along the species distribution, although present genetic structure largely confirms their permeability to gene flow. The Drâa valley marks the limit of the admixture between the southern and northern clusters, as signs of admixture are essentially absent north of the Drâa. This is also revealed by the lack of mtDNA haplotype sharing at both valley sides and the identification of a third genetic deme north of the Drâa valley. This valley holds cryptic diversity in other reptiles adapted to Mediterranean conditions, such as *Mauremys leprosa* (Veríssimo et al., 2016) and *Daboia mauritanica* (Martínez-Freiría et al., 2017) thus, reinforcing its role as gene flow barrier.

Inland populations (e.g. Smara and Adrar Souttouff) seem to be currently isolated from coastal populations by unsuitable areas for *A. aureus*. The only mtDNA haplotype found in this area (CL1) is common to the coastal-central populations (windows 3 and 4), and also found in the southern and northern distribution of the species (Figure 4), suggesting colonization events of inland regions from central-coastal populations. In particular, specimens from Smara are assigned to the *C-I* lineage with no signals of admixture with the neighbour genetic group K1 (northern genetic deme), which reinforce the hypothesis of a regional south-north colonization axis.

5 | CONCLUSIONS

Our findings bring new and important insights into the Atlantic Sahara corridor hypothesis, highlighting its role both as centre of lineage diversification and as a biogeographic corridor for *A. aureus* dispersal, which is in line with other biogeographic corridors for other non-xeric reptiles across the African continent (e.g. Gonçalves et al., 2012, 2017; Kissling, Blach-Overgaard, Zwaan, & Wagner, 2016). Diversification within *A. aureus* likely occurred during regional climatic oscillations, largely caused by putative refugia in stable climatic areas. Subsequent population expansions following an increase in habitat suitability for the species during the LGM, and after the mid-Holocene, facilitated migration events that resulted in interrupted gene flow dynamics and patterns of introgression along central populations, likely mediated by male-biased dispersal. Historical and contemporary genetic structure indicates geographical barriers to gene flow still persist.

DATA ACCESSIBILITY

GenBank accession numbers are the following: MG309921–MG310049 (12S), MG310096–MG310113 (COI), MG310114–MG310149 (Cytb) and MG310050–MG310095 (C-mos). The microsatellite dataset, 12S dataset and the analysis code to run the sliding window analysis can be found on GitHub at https://github.com/PJADPereira/slidinghet.

ORCID

Guillermo Velo-Antón http://orcid.org/0000-0002-9483-5695

REFERENCES

Alvarado-Serrano, D. F., & Knowles, L. L. (2014). Ecological niche models in phylogeographic studies: Applications, advances and precautions. *Molecular Ecology Resources*, 14, 233–248. https://doi.org/10.1111/1755-0998.12184

Anderson, R. P., & Raza, A. (2010). The effect of the extent of the study region on GIS models of species geographic distributions and estimates of niche evolution: Preliminary tests with montane rodents (genus *Nephelomys*) in Venezuela. *Journal of Biogeography*, 37, 1378–1393. https://doi.org/10.1111/j.1365-2699.2010.02290.x

Barbet-Massin, M., Jiguet, F., Albert, C. H., & Thuiller, W. (2012). Selecting pseudo–absences for species distribution models: How, where and how many? *Methods in Ecology and Evolution*, 3, 327–338. https://doi.org/10.1111/j.2041-210X.2011.00172.x

Belkhir, K., Borsa, P., Chikhi, L., Raufaste, N., & Bonhomme, F. (2004). *GENETIX 4.05, logiciel sous Windows TM pour la génétique des populations*. Montpellier, France: Laboratoire Génome, Populations, Interactions, CNRS UMR 5000, Université de Montpellier II. Retrieved from http://kimura.univ-montp2.fr/genetix/.

Bonnet, T., Leblois, R., Rousset, F., & Crochet, P.-A. (2017). A reassessment of explanations for discordant introgressions of mitochondrial and nuclear genomes. *Evolution*, 71, 2140–2158. https://doi.org/10.1111/evo.13296

Brito, J., Godinho, R., Martínez-Freiría, F., Pleguezuelos, J., Rebelo, H., Santos, X., . . . Carranza, S. (2014). Unravelling biodiversity, evolution and threats to conservation in the Sahara-Sahel. *Biological Reviews*, 89, 215–231. https://doi.org/10.1111/brv.12049

Brito, J. C., Tarroso, P., Vale, C. G., Martínez-Freiría, F., Boratyński, Z., Campos, J. C., . . . Carvalho, S. B. (2016). Conservation biogeography of the Sahara-Sahel: Additional protected areas are needed to secure unique biodiversity. *Diversity & Distributions*, 22, 371–384. https://doi.org/10.1111/ddi.12416

Boria, R. A., Olson, L. E., Goodman, S. M. & Anderson, R. P. (2014). Spatial filtering to reduce sampling bias can improve the performance of ecological niche models. *Ecological Modelling*, 275, 3–77. https://doi.org/10.1016/j.ecolmodel.2013.12.012

Carnaval, A. C., Hickerson, M. J., Haddad, C. F., Rodrigues, M. T., & Moritz, C. (2009). Stability predicts genetic diversity in the Brazilian Atlantic forest hotspot. *Science*, 323, 785–789. https://doi.org/10.1126/science.1166955

Carranza, S., & Arnold, E. N. (2012). A review of the geckos of the genus *Hemidactylus* (Squamata: Gekkonidae) from Oman based on morphology, mitochondrial and nuclear data, with descriptions of eight new species. *Zootaxa*, 3378, 1–95.

Carranza, S., Arnold, E. N., Geniez, P., Roca, J., & Mateo, J. A. (2008). Radiation, multiple dispersal and parallelism in the skinks, *Chalcides* and *Sphenops* (Squamata: Scincidae), with comments on *Scincus* and *Scincopus* and the age of the Sahara Desert. *Molecular Phylogenetics and Evolution*, 46, 071–094.

Clement, M., Posada, D. C., & Crandall, K. A. (2000). TCS: A computer program to estimate gene genealogies. *Molecular Ecology*, 9, 1657–1659. https://doi.org/10.1046/j.1365-294x.2000.01020.x

Crochet, P. A., Geniez, P., & Ineich, I. (2003). A multivariate analysis of the fringe-toed lizards of the Acanthodactylus scutellatus group (Squamata: Lacertidae): Systematic and biogeographical implications. *Zoological Journal of the Linnean Society*, 137, 117–155. https://doi.org/10.1046/j.1096-3642.2003.00044.x

Darriba, D., Taboada, G. L., Doallo, R., & Posada, D. (2012). jModelTest 2: More models, new heuristics and parallel computing. *Nature Methods*, 9, 772. https://doi.org/10.1038/nmeth.2109

Dinerstein, E., Olson, D., Joshi, A., Vynne, C., Burgess, N. D., Wikramanayake, E., . . . Hansen, M. (2017). An ecoregion-based approach to protecting half the terrestrial realm. *BioScience*, 67, 534–545. https://doi.org/10.1093/biosci/bix014

Douady, C. J., Catzeflis, F., Raman, J., Springer, M. S., & Stanhope, M. J. (2003). The Sahara as a vicariant agent, and the role of Miocene climatic events, in the diversification of the mammalian order Macroscelidea (elephant shrews). *Proceedings of the National Academy of Sciences*, 100, 8325–8330. https://doi.org/10.1073/pnas.0832467100

Drummond, A. J., Suchard, M. A., Xie, D., & Rambaut, A. (2012). Bayesian phylogenetics with BEAUti and the BEAST 1.7. *Molecular Biology and Evolution*, 29, 1969–1973. https://doi.org/10.1093/molbev/mss075

Duckett, P. E., Wilson, P. D., & Stow, A. J. (2013). Keeping up with the neighbours: Using a genetic measurement of dispersal and species distribution modelling to assess the impact of climate change on an Australian arid zone gecko (*Gehyra variegata*). *Diversity and Distributions*, 19, 964–976. https://doi.org/10.1111/ddi.12071

Earl, D. A. (2012). STRUCTURE HARVESTER: a website and program for visualizing STRUCTURE output and implementing the Evanno method. *Conservation genetics resources*, 4(2), 359–361. https://doi.org/10.1007/s12686-011-9548-7

Elith, J., Kearney, M., & Phillips, S. (2010). The art of modelling range-shifting species. *Methods in Ecology and Evolution*, 1, 330–342. https://doi.org/10.1111/j.2041-210X.2010.00036.x

ESRI. (2006). *ArcMap 9.2*. Redlands, CA: Environmental Systems Research Institute, Inc.

Evanno, G., Regnaut, S., & Goudet, J. (2005). Detecting the number of clusters of individuals using the software STRUCTURE: A simulation study. *Molecular Ecology*, 14, 2611–2620. https://doi.org/10.1111/j.1365-294X.2005.02553.x

Falush, D., Stephens, M., & Pritchard, J. K. (2003). Inference of population structure using multilocus genotype data: Linked loci and correlated allele frequencies. *Genetics*, 164, 1567–1587.

Ferchaud, A. L., Eudeline, R., Arnal, V., Cheylan, M., Pottier, G., Leblois, R., & Crochet, P. A. (2015). Congruent signals of population history but radically different patterns of genetic diversity between mitochondrial and nuclear markers in a mountain lizard. *Molecular Ecology*, 24, 192–207. https://doi.org/10.1111/mec.13011

Gonçalves, D. V., Brito, J. C., Crochet, P. A., Geniez, P., Padial, J. M., & Harris, D. J. (2012). Phylogeny of North African Agama lizards (Reptilia: Agamidae) and the role of the Sahara desert in vertebrate speciation. *Molecular Phylogenetics and Evolution*, 64, 582–591. https://doi.org/10.1016/j.ympev.2012.05.007

Gonçalves, D. V., Martínez-Freiría, F., Crochet, P. A., Geniez, P., Carranza, S., & Brito, J. C. (2017). The role of climatic cycles and trans-Saharan migration corridors in species diversification: Biogeography of *Psammophis schokari* group in North Africa. *Molecular Phylogenetics and Evolution*, 118, 64–74.

Graham, M. R., Jaeger, J. R., Prendini, L., & Riddle, B. R. (2013). Phylogeography of the Arizona hairy scorpion (*Hadrurus arizonensis*) supports a model of biotic assembly in the Mojave Desert and adds a

new Pleistocene refugium. *Journal of Biogeography*, 40, 1298–1312. https://doi.org/10.1111/jbi.12079

Hesse, P. P., Magee, J. W., & van der Kaars, S. (2004). Late Quaternary climates of the Australian arid zone: A review. *Quaternary International*, 118, 87–102. https://doi.org/10.1016/S1040-6182(03)00132-0

Hijmans, R. J., Cameron, S. E., Parra, J. L., Jones, P. G., & Jarvis, A. (2005). Very high resolution interpolated climate surfaces for global land areas. *International Journal of Climatology*, 25, 1965–1978. https://doi.org/10.1002/(ISSN)1097-0088

Irwin, D. E. (2002). Phylogeographic breaks without geographic barriers to gene flow. *Evolution*, 56(12), 2383–2394. https://doi.org/10.1554/0014-3820(2002)056[2383:PBWGBT]2.0.CO;2

Kearns, A. M., Joseph, L., Toon, A., & Cook, L. G. (2014). Australia's arid-adapted butcherbirds experienced range expansions during Pleistocene glacial maxima. *Nature communications*, 5, 3994.

Kissling, W. D., Blach-Overgaard, A., Zwaan, R. E., & Wagner, P. (2016). Historical colonization and dispersal limitation supplement climate and topography in shaping species richness of African lizards (Reptilia: Agaminae). *Scientific Reports*, 6, 34014.

Librado, P., & Rozas, J. (2009). DnaSP v5: A software for comprehensive analysis of DNA polymorphism data. *Bioinformatics*, 25, 1451–1452. https://doi.org/10.1093/bioinformatics/btp187

Liu, C., Berry, P. M., Dawson, T. P., & Pearson, R. G. (2005). Selecting thresholds of occurrence in the prediction of species distributions. *Ecography*, 28, 385–393. https://doi.org/10.1111/j.0906-7590.2005.03957.x

Lomolino, M. V., Riddle, B. R., Brown, J. H., & Brown, J. H. (2006). *Biogeography (No. QH84 L65 2006)*. Sunderland, MA: Sinauer Associates.

Lopes, S. C., Velo-Antón, G., Pereira, P., Lopes, S., Godinho, R., Crochet, P.-A., & Brito, J. C. (2015). Development and characterization of polymorphic microsatellite loci for spiny-footed lizards, *Acanthodactylus scutellatus* group (Reptilia, Lacertidae) from arid regions. *BMC Research Notes*, 8, 794. https://doi.org/10.1186/s13104-015-1779-3

Martínez-Freiría, F., Crochet, P.-A., Fahd, S., Geniez, P., Brito, J. C., & Velo-Antón, G. (2017). Integrative phylogeographic and ecological analyses reveal multiple Pleistocene refugia for Mediterranean *Daboia* vipers in North-West Africa. *Biological Journal of the Linnean Society*, 122(2), 366–384. https://doi.org/10.1093/biolinnean/blx038

Martínez-Freiría, F., Velo-Antón, G., & Brito, J. C. (2015). Trapped by climate: Interglacial refuge and recent population expansion in the endemic Iberian adder *Vipera seoanei*. *Diversity and Distributions*, 21, 331–344. https://doi.org/10.1111/ddi.12265

Ndiaye, A., Ba, K., Aniskin, V., Benazzou, T., Chevret, P., Konečný, A., … Granjon, L. (2012). Evolutionary systematics and biogeography of endemic gerbils (Rodentia, Muridae) from Morocco: An integrative approach. *Zoologica Scripta*, 41, 11–28. https://doi.org/10.1111/j.1463-6409.2011.00501.x

Otto-Bliesner, B. L., Marshall, S. J., Overpeck, J. T., Miller, G. H., & Hu, A. (2006). Simulating arctic climate warmth and icefield retreat in the last interglaciation. *Science*, 311, 1751–1753. https://doi.org/10.1126/science.1120808

Sindaco, R., & Jeremčenko, V. K. (2008). *The Reptiles of the Western Palearctic: Annotated checklist and distributional atlas of the turtles, crocodiles, amphisbaenians and lizards of Europe, North Africa, Middle East and Central Asia* (p. 579). Latina: Edizioni Belvedere.

Strasburg, J. L., Kearney, M., Moritz, C., & Templeton, A. R. (2007). Combining phylogeography with distribution modeling: Multiple Pleistocene range expansions in a parthenogenetic gecko from the Australian arid zone. *PLoS ONE*, 2, 1–20.

Stuut, J. B. W., & Lamy, F. (2004). Climate variability at the southern boundaries of the Namib (southwestern Africa) and Atacama (northern Chile) coastal deserts during the last 120,000 yr. *Quaternary Research*, 62, 301–309. https://doi.org/10.1016/j.yqres.2004.08.001

Tamar, K., Carranza, S., Sindaco, R., Moravec, J., Trape, J.-F., & Meiri, S. (2016). Out of Africa: Phylogeny and biogeography of the widespread genus *Acanthodactylus* (Reptilia: Lacertidae). *Molecular Phylogenetics and Evolution*, 103, 6–18. https://doi.org/10.1016/j.ympev.2016.07.003

Tamura, K., Stecher, G., Peterson, D., Filipski, A., & Kumar, S. (2013). MEGA6: Molecular evolutionary genetics analysis version 6.0. *Molecular Biology and Evolution*, 30, 2725–2729. https://doi.org/10.1093/molbev/mst197

Tchakerian, V. P., & Lancaster, N. (2002). Late Quaternary arid/humid cycles in the Mojave Desert and western Great Basin of North America. *Quaternary Science Reviews*, 21, 799–810. https://doi.org/10.1016/S0277-3791(01)00128-7

Thuiller, W., Georges, D., & Engler, R. (2012). Package "biomod 2" version 2.1.15. Retrieved from http://cran.r-project. org/web/packages/biomod2/biomod2.pdf (accessed 11 June 2015).

Toews, D. P., & Brelsford, A. (2012). The biogeography of mitochondrial and nuclear discordance in animals. *Molecular Ecology*, 21, 3907–3930. https://doi.org/10.1111/j.1365-294X.2012.05664.x

Trape, S. (2009). Impact of climate change on the relict tropical fish fauna of Central Sahara: Threat for the survival of Adrar mountains fishes, Mauritania. *Plos ONE*, 4, e4400. https://doi.org/10.1371/journal.pone.0004400

Trape, J. F., Trape, S., & Chirio, L. (2012). *Lézards, crocodiles et tortues d'Afrique occidentale et du Sahara*. France: IRD éditions.

Vale, C. G., Pimm, S. L., & Brito, J. C. (2015). Overlooked mountain rock pools in deserts are critical local hotspots of biodiversity. *PLoS ONE*, 10, e0118367. https://doi.org/10.1371/journal.pone.0118367

Van Oosterhout, C., Hutchinson, W. F., Wills, D. P., & Shipley, P. (2004). MICRO-CHECKER: Software for identifying and correcting genotyping errors in microsatellite data. *Molecular Ecology Notes*, 4, 535–538. https://doi.org/10.1111/j.1471-8286.2004.00684.x

Veríssimo, J., Znari, M., Stuckas, H., Fritz, U., Pereira, P., Teixeira, J., … Velo-Antón, G. (2016). Pleistocene diversification in Morocco and recent demographic expansion in the Mediterranean pond turtle *Mauremys leprosa*. *Biological Journal of the Linnean Society*, 119, 943–959.

Vogel, P., Mehmeti, A. M., Dubey, S., Vogel-Gerber, C., Koyasu, K., & Ribi, M. (2006). Habitat, morphology and karyotype of the Saharan shrew *Crocidura tarfayaensis* (Mammalia: Soricidae). *Acta Theriologica*, 51, 353–361. https://doi.org/10.1007/BF03195182

Ward, D. (2009). *Biology of deserts*. Oxford, UK: Oxford University Press.

Watrin, J., Lézine, A. M., & Hély, C. (2009). Plant migration and plant communities at the time of the "green Sahara". *Comptes Rendus Geoscience*, 341, 656–670. https://doi.org/10.1016/j.crte.2009.06.007

Wiens, J. A., Stralberg, D., Jongsomjit, D., Howell, C. A., & Snyder, M. A. (2009). Niches, models, and climate change: Assessing the assumptions and uncertainties. *Proceedings of the National Academy of Sciences*, 106, 19729–19736. https://doi.org/10.1073/pnas.0901639106

Worth, J. R., Williamson, G. J., Sakaguchi, S., Nevill, P. G., & Jordan, G. J. (2014). Environmental niche modelling fails to predict Last Glacial Maximum refugia: Niche shifts, microrefugia or incorrect palaeoclimate estimates? *Global Ecology and Biogeography*, 23, 1186–1197. https://doi.org/10.1111/geb.12239

BIOSKETCH

Guillermo Velo-Antón is an Associate Researcher at CIBIO-InBIO (University of Porto, Portugal) and a molecular ecologist studying how eco-evolutionary processes operate at different time scales. All authors are members of BIODESERTS (http://biodeserts.cibio.up.pt/).

Author contributions: G.V.A., P.A.C. and J.C.B. conceived the study; J.C.B., F.M.F., P.A.C. and G.V.A. performed the sampling; G.V.A., F.M.F. and P.P. analysed the data; G.V.A. wrote the manuscript with important contributions from co-authors.

SUPPORTING INFORMATION

Additional Supporting Information may be found online in the supporting information tab for this article.